

Soil CO₂ emission estimated by different interpolation techniques

Daniel De Bortoli Teixeira · Alan Rodrigo Panosso ·
Carlos Eduardo Pelegrino Cerri · Gener Tadeu Pereira · Newton La Scala Jr.

Received: 10 May 2010 / Accepted: 9 March 2011 / Published online: 19 April 2011
© Springer Science+Business Media B.V. 2011

Abstract Soil CO₂ emissions are highly variable, both spatially and across time, with significant changes even during a one-day period. The objective of this study was to compare predictions of the diurnal soil CO₂ emissions in an agricultural field when estimated by ordinary kriging and sequential Gaussian simulation. The dataset consisted of 64 measurements taken in the morning and in the afternoon on bare soil in southern Brazil. The mean soil CO₂ emissions were significantly different between the morning ($4.54 \mu\text{mol m}^{-2} \text{s}^{-1}$) and afternoon ($6.24 \mu\text{mol m}^{-2} \text{s}^{-1}$) measurements. However, the spatial variability structures were similar, as the models were spherical and had close range values of 40.1 and 40.0 m for the morning and afternoon semivariograms. In both periods, the sequential Gaussian simulation maps were more efficient for

the estimations of emission than ordinary kriging. We believe that sequential Gaussian simulation can improve estimations of soil CO₂ emissions in the field, as this property is usually highly non-Gaussian distributed.

Keywords Soil respiration · Geostatistics · Ordinary kriging · Sequential gaussian simulation

Introduction

Measurement of soil CO₂ emissions (FCO₂) in agricultural areas is an important tool, especially when high levels of temporal and spatial variability are observed. FCO₂ is highly variable in space and time; this is true even in bare soils, where labile carbon decomposition is the only source. Attempts to describe the temporal variability of FCO₂ in several ecological systems have focused on soil temperature and soil moisture (Schwendenmann et al. 2003; Epron et al. 2004; Kosugi et al. 2007), especially in temperate climates (Scott-Denton et al. 2003; Shi et al. 2006; Flechard et al. 2007, Martin et al. 2009). In terms of its spatial variability, FCO₂ is controlled by many properties; these are mostly physical, e.g., soil porosity and texture (Dilustro et al. 2005). Few works have attempted to relate soil CO₂ emissions and soil temperature or soil moisture in terms of spatial variability. Soil temperature and moisture are the main factors affecting microbial activity, although

Responsible Editor: Ute Skiba.

D. De Bortoli Teixeira (✉) · A. R. Panosso ·
G. T. Pereira · N. La Scala Jr.
Departamento de Ciências Exatas—FCAV/UNESP,
Universidade Estadual Paulista,
Via de Acesso Prof. Paulo Donato Castellane s/n.,
14884–900 Jaboticabal, SP, Brazil
e-mail: danieldbt@bol.com.br

C. E. P. Cerri
Departamento de Ciência do Solo—ESALQ/USP,
Universidade de São Paulo,
Av. Páduas Dias, 11, CP. 9,
13418–900 Piracicaba, SP, Brazil

other aspects (such as organic matter, pH, cation exchange capacity and the oxygen level of the soil) could also be related to this activity (Fang et al. 1998; La Scala Jr et al. 2000; Savin et al. 2001; Saiz et al. 2006; Cerri et al. 2006). Most of the physical, chemical (Webster 1985; Webster and Oliver 1990; Cambardella et al. 1994; Wang et al. 2002) and biological properties (Sinegani et al. 2005; Konda et al. 2008) that are possibly related to soil CO₂ emissions have been considered to have a spatial variability structure. Hence, it is expected that FCO₂ also presents a well-defined spatial variability structure, and this idea has been shown in some recent works (La Scala Jr et al. 2003; Herbst et al. 2009; Panosso et al. 2009). Due to the complexity of the spatial variability structure of FCO₂, understanding the soil-carbon balance in agricultural areas is an important task that should be addressed in a quantitative way using appropriate tools. Modeling spatial dependence through geostatistics is one of the tools that have been applied to describe the spatial variability of soil CO₂ emissions (Panosso et al. 2009).

The ordinary kriging (OK) and sequential Gaussian simulation (SGS) are two geostatistical techniques that have the same goal: to estimate the soil properties in non-sampled points by characterizing its spatial distribution on a certain area using real measurements conducted on a limited number of points. The kriging algorithm is focused on providing the “best” (defined in a minimized least squares sense), and hence it is a unique, local estimate of a variable without specific regard for the resulting spatial statistics of all of the estimates taken together (Deutsch and Journel 1998). In studies conducted by Wang et al. (2001), SGS has also been applied to assess the uncertainty of the soil erodibility. Juang et al. (2004) assessed this uncertainty by applying SGS to studies of soils that were contaminated with heavy metals. A stochastic simulation procedure based on SGS has also been used to map FCO₂ in volcanic areas (Cardellini et al. 2003; Lewicki et al. 2005). Those studies have concluded that the SGS method produces more realistic representations than a more traditional estimation technique, ordinary kriging, especially for the description of FCO₂ in volcanic areas. Therefore, SGS has increasingly been applied as an alternative to kriging and is preferred for applications in which the spatial variation of the measured field must be preserved (Srivastava 1996).

Despite these efforts, few works have focused on determining the best method to estimate FCO₂ in locations that were not sampled (Lewicki et al. 2005). In this work, we tested two different interpolation methods, ordinary kriging and sequential Gaussian simulation, to validate the best method for estimating FCO₂ in an agricultural area in the southern region of Brazil.

Material and methods

The work was conducted on the FCAV/UNESP experimental farm (21°15' S 48°18' W) in the southern region of Brazil, where the soil is classified as Eutroferic red Latosol (Oxisol). Meteorological data indicates a mean annual precipitation of 1,425 mm that is concentrated from October to March, with few precipitation events from April to September. Two days before the CO₂ emission measurements, the soil was tilled with a disk plow at a depth of 0.20 m. After tillage, 64 points were defined in the soil, forming an irregular grid with a minimum distance of 5 m between points, covering an area of 110×15 m.

The soil CO₂ emissions (FCO₂) were measured using a LI-8100 produced by Li-Cor (Nebraska, USA). Emissions were studied during the morning and the afternoon of March 31, 2007, in two events: from 7:30 to 10:30 (morning) and from 13:50 to 16:50 (afternoon).

The variability of FCO₂ was first described applying descriptive statistics (mean ± standard error, standard deviation, coefficient of variation, minimum, maximum, skewness, kurtosis and normality test) and after by spatial variability (magnitude and direction) using experimental semivariogram modeling. The experimental semivariogram is derived by the following relation:

$$\hat{\gamma}(h) = \frac{1}{2N(h)} \sum_{i=1}^{N(h)} [z(x_i) - z(x_i + h)]^2 \quad (1)$$

As $\hat{\gamma}(h)$ is the experimental semivariance for a separation distance h , $z(x_i)$ is the property value FCO₂ at the i th point, and $N(h)$ is the number of pairs of points separated by distance h . The process of kriging and sequential Gaussian simulation starts with a model adjustment to the experimental semivariogram

(C_0 , C_0+C_1 and a). Those parameters are known as the nugget effect (C_0), the sill (C_0+C_1) and the range (a). The nugget effect is the sum of two components of measurement error: the sampling error and the error due to short scale variability, i.e., the variability of the observations separated by a distance that is smaller than the minimum distance used in the grid (Isaaks and Srivastava 1989). The sill is the point at which the semivariogram model stabilizes and approximately describes the variance of the studied data. The range is the distance at which this stabilization occurs and from where data can be considered spatially independent.

Spherical, exponential and Gaussian models are valid and can be used to describe the experimental semivariogram. The spherical model is given by:

$$\hat{\gamma}(h) = C_0 + C_1 \left[\frac{3}{2} \left(\frac{h}{a} \right) - \frac{1}{2} \left(\frac{h}{a} \right)^3 \right]; \text{ if } 0 < h < a \quad (2)$$

$$\text{And } \hat{\gamma}(h) = C_0 + C_1; \text{ for } h \geq a \quad (3)$$

The Exponential model;

$$\hat{\gamma}(h) = C_0 + C_1 \left[1 - \exp \left(-3 \frac{h}{a} \right) \right]; \text{ if } 0 < h < d \quad (4)$$

The Gaussian model:

$$\hat{\gamma}(h) = C_0 + C_1 \left[1 - \exp \left(-3 \left(\frac{h}{a} \right)^2 \right) \right]; \text{ if } 0 < h < d \quad (5)$$

with d being the semivariogram maximum distance.

Each semivariogram model describes a spatial variability with different characteristics. The spherical model reaches sill more quickly than the Gaussian model, indicating that the data show a lower erraticity and are not continuously presented in the study field; however, in the Gaussian model, the data usually have a high spatial correlation over smaller distances.

Ordinary kriging, the first method tested, is found by summing the adjacent samples (Eq. 6); the weight of each sample is determined using the data structural correlation to reduce the estimated variance (Lin 2008). Estimation of the non-sampled points is based on the sampled data, and in the semivariogram model parameters, the best representation of the spatial correlation of the sampled data. Although kriging is considered to be the best linear unbiased estimate

(BLUE), this technique promotes the smoothing of data, overestimating lower values and underestimating higher values.

$$z^*(x_0) = \sum_{i=1}^N \lambda_i z(x_i) \quad (6)$$

where $z^*(x_0)$ is the estimated value of the property in x_0 , N is the number of values applied in the estimation, λ_i is the weight associated to each value and $z(x_i)$ is the measured value of the property at the i th point.

However, sequential Gaussian simulation generates several equally probable maps. The realization of SGS is as follows: (1) normalization of the observed values (with mean and variance being equal to 0 and 1, respectively), (2) semivariogram determination using the normalized values, (3) refinement of the sampled grid, (4) definition of a random path that is capable of passing through all of the non-sampled points in the grid area, (5) random choice of the node in the sampled grid, (6) estimation by kriging of the selected node (deriving the estimated value and its variance), (7) a normal distribution based on the data derived in step 6, (8) the cumulative distribution function is calculated, (9) removal of a random observed values of this function, (10) this value is chosen to represent the studied property in the same spot from which it was removed, (11) repetition of the 5–9 procedure until visiting all of the observed points, (12) repetition of the 4–11 procedure until all of the realizations have been performed and (13) transformation of the obtained values for the mean and variance of the original data. After all of the steps, SGS generates a mean map of those n realizations for the studied property (FCO2).

The FCO2 values were estimated and simulated using OK and SGS to form a refined grid with 166 columns \times 22 lines, with a total of 3,652 points separated by a regular distance of 0.67 m. Pearson analysis was conducted to compare the estimated and simulated values across the 3,652 points of maps generated by both techniques.

To identify the most efficient method for estimating FCO2 in the field, maps were generated and submitted to external validation that compares the actual data (collected in the field) with the estimated results from both approaches (ordinary kriging and sequential Gaussian simulation). In our study, we separated about 10% of the total data points for the external validation

Table 1 Descriptive statistics of soil CO₂ emission (μmol m⁻²s⁻¹) in the morning and in the afternoon

Period	Mean	SE	SD	CV	Min	Max	Skew	Kurt	Normality test (<i>p</i>)
Fmorning	4.54	0.20	1.57	34.55	1.67	8.77	0.72	0.12	0.03
Fafternoon	6.24	0.27	2.17	34.77	2.98	12.77	1.09	1.10	<0.01

N=64; *SE* Standard Error; *SD* Standard Deviation; *CV* Coefficient of Variation (%); *Min* Minimum; *Max* Maximum; *Skew* Skewness; *Kurt* Kurtosis. Normality Test according of the Cramer-von Mises test

(in our case, 5 out of 64 sampled points), and the remaining 90% were used for the variographic analyses (Cerri et al. 2004). Those 5 points were randomly selected within the sampling grid, avoiding points at the edge of the grid to assure the highest possible number of close neighbors. External validation analysis was assessed based on the mean error (ME) and root mean square error (RMSE) (Bourennane et al. 2000; Bourennane and King 2003; Cerri et al. 2004; Bourennane et al. 2007; Chai et al. 2007; Chirico et al. 2007) given by following equations:

$$ME = \frac{1}{n} \sum_{i=1}^n [z(x_i) - z^*(x_i)] \quad (7)$$

$$RMSE = \left\{ \frac{1}{n} \sum_{i=1}^n [z(x_i) - z^*(x_i)]^2 \right\}^{0.5} \quad (8)$$

where *n* is the number of values used in the validation, *z*(*x_i*) is the FCO₂ value at the *i*th point, and *z*^{*}(*x_i*) is the estimated/simulated FCO₂ value at point *i*. For non-biased methods, ME should be close to zero, while higher accuracy is related to smaller RSME values.

The software GS+, version 7 (Gamma Design Software 1998), was used to adjust the semivariograms and perform kriging and sequential Gaussian simulation; the maps were developed by Surfer software, Version 8 (SURFER for Windows 1995).

Table 2 Semivariogram parameters and coefficient of determination (*R*²) for FCO₂ in the morning and afternoon periods, fitted using spherical models

	<i>C</i> ₀	<i>C</i> ₀ + <i>C</i> ₁	<i>A</i> (m)	<i>C</i> ₀ / <i>(C</i> ₀ + <i>C</i> ₁)	<i>R</i> ²
Fmorning	0.559	2.750	40.10	0.20	0.83
Fafternoon	0.900	5.982	40.00	0.15	0.88

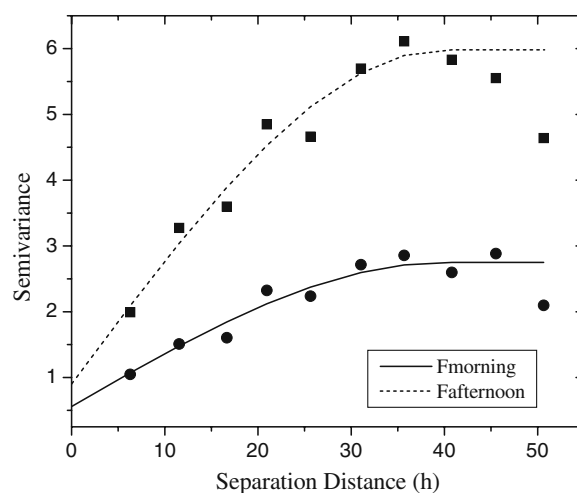
N=59

Results

The mean value of soil CO₂ emissions in the morning was 4.54 ± 0.20 μmol m⁻²s⁻¹, significantly (paired Student's *t*-test; *p*<0.01) smaller than the value observed in the afternoon, 6.24 ± 0.27 μmol m⁻²s⁻¹ (Table 1). In both of the periods, high values of the coefficient of variation (34.55 and 34.77 for the morning and afternoon, respectively) were observed; this was the first indication that FCO₂ spatial variability must be considered (Panosso et al. 2009).

Table 2 presents the parameters of the variogram models for FCO₂ during the morning and afternoon observation periods. The range values were similar (Fig. 1), both periods presented strong spatial dependence, as verified by the *C*₀/*(C*₀+*C*₁) ratio <0.25 (Cambardella et al. 1994).

To perform the estimate using SGS, it is necessary to define the number of realizations that will be used in the process. A small amount of simulations generates irregular maps, but a great number of realizations in SGS cause the mean map to converge to one that is close to the kriging (Robertson 2008;

**Fig. 1** Semivariograms fitted using spherical models for FCO₂ in morning (—●—) and afternoon (—■—) periods

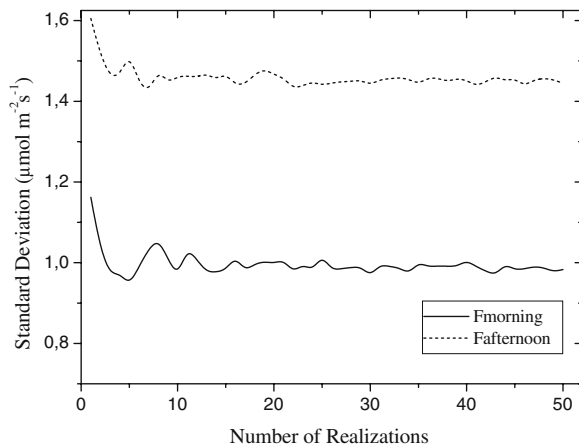


Fig. 2 Standard deviation of FCO₂ as a function of the number of simulations when estimated by SGS in the morning (—) and in the afternoon (---)

Bourennane et al. 2007; Chai et al. 2007). Figure 2 presents the mean standard deviation of the generated map after each SGS realization (mean map of those n realizations). Examining the standard deviation values enable us to compare the accuracy and precision of the simulated maps (Bourennane et al. 2007), as smaller standard deviations imply higher interpolation accuracy and precision. The afternoon period presented higher values of the standard deviation. Noticeably, an increase in the realization number for SGS resulted in a rapid decrease in the standard deviation values that had stabilized close to 20 realizations in both periods, with values of 1.45 and $0.99 \mu\text{mol m}^{-2}\text{s}^{-1}$ for the afternoon and morning, respectively (Fig. 2). Those standard deviation values are similar to the ones found in ordinary kriging (Table 3). Therefore, we can assume that estimates

above 20 realizations in SGS were enough for our FCO₂ simulation.

Table 3 presents the descriptive statistics of the observed and estimated values of FCO₂ (morning and afternoon) when estimated by ordinary kriging and SGS. For all cases, 48 neighbors were considered in the estimation of each non-sampled point. The means determined using SGS were dissimilar when compared to OK, being closer to the original data values collected in the field. In both OK and SGS, 3,652 points were generated from the original 59 (not including the 5 points kept for the external validation procedure). Despite small changes in the mean values, standard deviation and CV, it is possible to notice that SGS produces better estimates than ordinary kriging for both morning and afternoon when the observed and estimated values are compared.

FCO₂ estimated maps in the morning and afternoon by both interpolation methods are presented in Fig. 3. Ordinary kriging generated a smooth map, without abrupt curves in the isolines, when compared to the SGS map. In both time periods, the ordinary kriging maps presented a high correlation with the SGS maps, 0.98 and 0.99 ($p < 0.001$) in the morning and afternoon, respectively. It is also worth noting that the points with high FCO₂ in the mornings also presented higher FCO₂ levels in the afternoon period.

The external validation (using FCO₂ measurements from the 5 points removed from grid) provides the opportunity to compare the observed and estimated data (Table 4). In both periods, the sequential Gaussian simulation performed better estimations than ordinary kriging, with smaller values of both the mean error and the root mean square error.

Table 3 Descriptive statistics of FCO₂ ($\mu\text{mol m}^{-2}\text{s}^{-1}$) observed data (grid) and data generated by ordinary kriging (OK) and sequential Gaussian simulation (SGS), in both periods (morning and afternoon)

Procedure	N	Mean	SD	CV	Skewness	Kurtosis
Morning period Grid (measured data)	64	4.54	1.57	34.55	0.72	0.12
OK	3652	4.42	0.98	22.26	0.37	-0.15
SGS 20	3652	4.47	1.00	22.35	0.36	-0.07
Afternoon period (measured data)	64	6.24	2.17	34.77	1.09	1.10
OK	3652	6.08	1.45	23.87	0.78	0.30
SGS 20	3652	6.14	1.47	23.89	0.81	0.42

SD Standard Deviation; CV Coefficient of Variations (%); N The number of observations

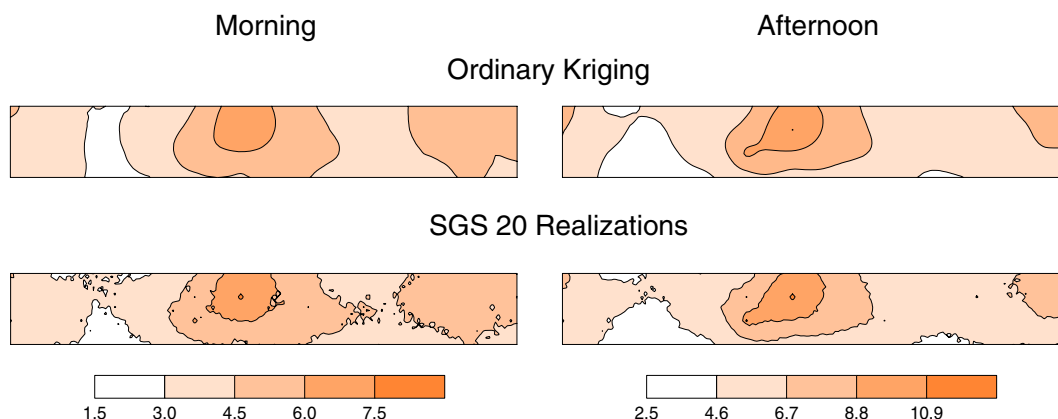


Fig. 3 Spatial patterns of FCO₂ ($\mu\text{mol m}^{-2} \text{s}^{-1}$) generated by different interpolation methods, ordinary kriging and sequential Gaussian simulation (SGS), for the morning and the afternoon periods

Discussion

In general, the FCO₂ levels were higher than those previously observed in similar studies conducted in our region in the same season (La Scala Jr et al. 2003). We believe that this effect was due to the proximity of soil tillage. Tillage is well known to induce soil carbon losses by CO₂ emission due not only to the increase in aeration but also the breakdown of aggregates, which exposes additional labile carbon to microbial activity (Six et al. 1999; La Scala Jr et al. 2009). The higher standard deviation and coefficient of variation (CV) values are of the same magnitude as those found by La Scala Jr et al. (2000) in a bare Oxisol. Epron et al. (2004) have also observed high FCO₂ CV values in a *Eucalyptus* plantation. Schwendenmann et al. (2003) found FCO₂ CV values between 35 and 45% in a tropical forest study.

Table 4 Validation of FCO₂ in morning and afternoon periods generated by ordinary kriging (OK) and sequential Gaussian simulation (SGS) using 20 simulations

	OK	SGS
Fmorning		
ME	0.57	0.37
RSME	1.26	1.22
Fafternoon		
ME	0.51	0.26
RSME	0.60	0.40

ME mean error and RMSE root mean square error

The higher C₀ values for the afternoon estimation imply a smaller precision in the FCO₂ estimates performed in this period, when compared to the morning (Isaaks and Srivastava 1989). The high range values (40.1 and 40.0 m in the morning and afternoon, respectively) are related to the soil management that promoted the homogeneity of the area. Some studies were not able to capture a spatial dependence of FCO₂, but the majority indicate values with ranges varying from a few meters up to 100 m (Stoyan et al. 2000; Rayment and Jarvis 2000; Lewicki et al. 2003; Ishizuka et al. 2005; Ohashi and Gyokusen 2007). Konda et al. (2008) found values ranging from 1.8 to 65 m for FCO₂ in an *Acacia mangium* plantation by changing the scale assessed from 1×1 to 10×10 m, respectively. In a study of bare soil conditions, La Scala Jr et al. (2000) observed a range of values from 29.6 m to 58.4 m. In a Southeast Asian tropical rainforest, Kosugi et al. (2007) found spherical models to be better adjusted to FCO₂, with emissions levels ranging from 4.4 to 24.7 m.

The number of realizations needed for the best estimations using SGS is still unknown for most soil properties. Lin (2008), who studied the spatial variability of arsenic in soil, verified that SGS above 100 realizations resulted in steady mean standard deviations. This result indicates the need to perform different map realizations (or representations) when applying the SGS technique in order to identify the number of realizations needed for the standard deviations to achieve stabilization.

The higher value of standard deviation in the afternoon could be justified by the higher C_0 value found for this period relative to the morning. As mentioned previously, higher C_0 values are directly related to an increase in the variance of the estimations and consequently an increase in the error of the estimation values.

One of the main advantages of SGS is a more consistent representation of the FCO₂ descriptive statistics (Table 3). The performance improvement of SGS could be related to the high asymmetry (skewness) or kurtosis of the observed data, especially in the afternoon, as ordinary kriging is more accurate when the results are closer to a normal distribution (Paz-Gonzalez et al. 2001). Our results are in agreement with those reported by Cardellini et al. (2003), who found that kriging was able to reproduce neither the histogram nor the variogram statistics of the diffuse soil CO₂ fluxes. Goovaerts (1999) reported that kriged maps should not be used for applications that are sensitive to the presence of extreme values because kriging cannot reproduce reliably basic statistics of the original data.

The ME values closer to zero found for SGS (Table 4) in both periods indicate that this technique produced a smaller bias than OK. Also, the RMSE values confirm that the SGS technique estimated the non-sampled points with higher accuracy. Compared to the OK method, the SGS method resulted in an improved accuracy of approximately 3% and 33% in the morning and afternoon periods, respectively. The higher precision in the afternoon is justified by the higher asymmetry of the measured values during this period (Table 1), confirming that the OK technique is unable to adequately estimate the observed values when the data does not form a normal distribution.

Conclusions

The spatial variability models of FCO₂ were similar in the morning and afternoon. FCO₂ presented a best representation when estimated by sequential Gaussian simulation, better than the representation estimated by ordinary kriging. This study verified that a rigorous statistical procedure is essential to better represent the non-sampled points closer to the real values observed in field. Such findings are useful for future studies, not only for CO₂ emissions but also potentially for

N₂O and CH₄ emissions. Moreover, they can enhance our understanding of the emission patterns of these important sources of greenhouse gases.

Acknowledgements We acknowledge FAPESP (Fundação de Amparo a Pesquisa do Estado de São Paulo) and CNPq (Conselho Nacional de Desenvolvimento Científico e Tecnológico), Brazil, for their financial support.

References

- Bourennane H, King D (2003) Using multiple external drifts to estimate a soil variable. *Geoderma* 114:1–18
- Bourennane H, King D, Couturier A (2000) Comparison of kriging with external drift and simple linear regression for predicting soil horizon thickness with different sample densities. *Geoderma* 97:255–271
- Bourennane H, King D, Couturier A, Nicoulaud B, Mary B, Richard G (2007) Uncertainty assessment of soil water content spatial patterns using geostatistical simulations: an empirical comparison of a simulation accounting for single attribute and a simulation accounting for secondary information. *Ecol Model* 205:323–335
- Cambardella CA, Moorman TB, Novak JM, Parkin TB, Karlen DL, Turco RF, Konopka AE (1994) Field-scale variability of soil properties in central Iowa soils. *Soil Sci Soc Am J* 58:1501–1511
- Cardellini C, Chiodini G, Frondini F (2003) Application of stochastic simulation to CO₂ flux from soil: mapping and quantification of gas release. *J Geophys Res* 108:2425
- Cerri CEP, Bernoux M, Volkoff B, Victoria RL, Melillo JM, Paustian K, Cerri CC (2004) Assessment of soil property spatial variation in an Amazon pasture: basis for selecting an agronomic experimental area. *Geoderma* 123:51–68
- Cerri CEP, Piccolo MC, Feigl BJ, Paustian K, Cerri CC, Victoria RL, Melillo JM (2006) Interrelationships among soil total C and N, microbial biomass, trace gas fluxes, and internal N-cycling in soils under pasture of the Amazon region. *J Sustain Agric* 27:45–69
- Chai X, Huang Y, Yuan X (2007) Accuracy and uncertainty of spatial patterns of soil organic matter. *New Zeal J Agric Res* 50:1141–1148
- Chirico GB, Medina H, Romano N (2007) Uncertainty in predicting soil hydraulic properties at the hillslope scale with indirect methods. *J Hydrol* 334:405–422
- Deutsch CV, Journel AG (1998) *GSLIB: Geostatistical Software Library: and user's guide*, 2nd edn. Oxford University Press, New York, p 369
- Dilustro JJ, Collins B, Duncan L, Crawford C (2005) Moisture and soil texture effects on soil CO₂ efflux components in southeastern mixed pine forests. *For Ecol Manag* 204:87–97
- Epron D, Nouvellon Y, Roupsard O, Mouvondy W, Mabiala A, Saint-André L, Joffre R, Jourdan C, Bonnefond JM, Berbigier P, Hamel O (2004) Spatial and temporal variations of soil respiration in a Eucalyptus plantation in Congo. *For Ecol Manag* 202:149–160

- Fang C, Moncrieff JB, Gholz HL, Clark KL (1998) Soil CO₂ efflux and its spatial variation in a Florida slash pine plantation. *Plant Soil* 205:135–146
- Flechar CR, Neftel A, Jocher M, Ammann C, Leifeld J, Fuhrer J (2007) Temporal changes in soil pore space CO₂ concentration and storage under permanent grassland. *Agric For Meteorol* 142:66–84
- Gamma Design Software (1998) GS+ geostatistics for the environmental sciences 3.07. Gamma Design Software, MI, USA
- Goovaerts P (1999) Geostatistics in soil science: state-of-the-art and perspectives. *Geoderma* 89:1–45
- Herbst M, Prolingheuer N, Graf A, Huisman JA, Weihermüller L, Vanderborght J (2009) Characterization and understanding of bare soil respiration spatial variability at plot scale. *Soil Sci Soc Am J* 8:762–771
- Isaaks EH, Srivastava RM (1989) Applied geostatistics. Oxford University Press, Nova York
- Ishizuka S, Iswandi A, Nakajima Y, Yonemura L, Sudo S, Tsuruta H, Muriyarso D (2005) Spatial patterns of greenhouse gas emissions in a tropical rainforest in Indonesia. *Nutr Cycl Agroecosyst* 71:55–62
- Juang KW, Chen YS, Lee DY (2004) Using sequential indicator simulation to assess the uncertainty of delineating heavy-metal contaminated soils. *Environ Pollut* 127:229–238
- Konda R, Ohta S, Ishizuka S, Arai S, Ansori S, Tanaka N, Hardjono A (2008) Spatial structures of N₂O, CO₂, and CH₄ fluxes from Acacia mangium plantation soils during a relatively dry season in Indonesia. *Soil Biol Biochem* 40:3021–3030
- Kosugi Y, Mitani T, Itoh M, Noguchi S, Tani M, Matsuo N, Takanashi S, Ohkubo S, Nik AR (2007) Spatial and temporal variation in soil respiration in a Southeast Asian tropical rainforest. *Agric For Meteorol* 147:35–47
- La Scala N Jr, Marques J Jr, Pereira GT, Corá JE (2000) Short-term temporal changes in the spatial variability model of CO₂ emissions from a Brazilian bare soil. *Soil Biol Biochem* 32:1459–1462
- La Scala N Jr, Pereira GT, Panosso AR (2003) Variabilidade espacial e temporal da emissão de CO₂ num agrossistema desprovido de vegetação. *Eng Agric* 23:88–95
- La Scala N Jr, Lopes A, Spokas K, Archer D, Reicosky DC (2009) Short-term temporal changes of bare soil CO₂ fluxes after tillage described by first-order decay models. *Eur J Soil Sci* 60:258–264
- Lewicki JL, Evans WC, Hilley GE, Sorey ML, Rogie JD, Brantley SL (2003) Shallow soil CO₂ flow along the San Andreas and Calaveras faults, CA. *J Geophys Res* 108:2187–2201
- Lewicki JL, Bergfeld D, Cardellini C, Chiodini G, Granieri D, Varley N, Werner C (2005) Comparative soil CO₂ flux measurements and geostatistical estimation methods on Masaya volcano, Nicaragua. *B Volcanol* 68:76–90
- Lin YP (2008) Simulating spatial distributions, variability and uncertainty of soil arsenic by geostatistical simulations in geographic information systems. *Open Environ J* 2:26–33
- Martin JG, Bolstad PV, Ryu SR, Chen J (2009) Modeling soil respiration based on carbon, nitrogen, and root mass across diverse Great Lake forests. *Agric For Meteorol* 149:1722–1729
- Ohashi M, Gyokusen B (2007) Temporal change in spatial variability of soil respiration on a slope of Japanese cedar (*Cryptomeria japonica* D. Don) forest. *Soil Biol Biochem* 39:1130–1138
- Panosso AR, Marques J Jr, Pereira GT, La Scala N Jr (2009) Spatial and temporal variability of soil CO₂ emission in a sugarcane area under green and slash-and-burn managements. *Soil Tillage Res* 105:275–282
- Paz-Gonzalez A, Taboada Castro MT, Vieira SR (2001) Geostatistical analysis of heavy metals in a one-hectare plot under natural vegetation in a serpentine area. *Can J Soil Sci* 81:469–479
- Rayment MB, Jarvis PG (2000) Temporal and spatial variation of soil CO₂ efflux in a Canadian boreal forest. *Soil Biol Biochem* 32:35–45
- Robertson GP (2008) GS+: geostatistics for the environmental sciences. Gamma Design Software, Plainwell
- Saiz G, Green C, Butterbach-Bahl K, Kiese R, Avitabile V, Farrell EP (2006) Seasonal and spatial variability of soil respiration in four Sitka spruce stands. *Plant Soil* 287:161–176
- Schwendenmann L, Veldkamp E, Brenes T, O'Brien JJ, Mackensen J (2003) Spatial and temporal variation in soil CO₂ efflux in an old-growth neotropical rain forest, La Selva, Costa Rica. *Biogeochemistry* 64:111–128
- Savin MC, Görres JH, Neher DA, Amador JA (2001) Biogeophysical factors influencing soil respiration and mineral nitrogen content in an old field soil. *Soil Biol Biochem* 33:429–438
- Scott-Denton LE, Sparks KL, Monson RK (2003) Spatial and temporal controls of soil respiration rate in a high-elevation, subalpine forest. *Soil Biol Biochem* 35:525–534
- Shi PL, Zhang XZ, Zhong ZM, Ouyang H (2006) Diurnal and seasonal variability of soil CO₂ efflux in a cropland ecosystem on the Tibetan Plateau. *Agric For Meteorol* 137:220–223
- Sinegani AAS, Mahboobi AA, Nazarizadeh F (2005) The effect of agricultural practices on the spatial variability of arbuscular mycorrhiza spores. *Turk J Biol* 29:149–153
- Six J, Elliott ET, Paustian K (1999) Aggregate and soil organic matter dynamics under conventional and no-tillage systems. *Soil Sci Soc Am J* 63:1350–1358
- Srivastava MR (1996) An overview of stochastic simulation. In: Mowrer HT, Czaplewski RL, Hamre RH (eds) Spatial accuracy assessment in natural resources and environmental sciences: Second Int. Symposium. U.S. Dept. of Agriculture, Forest Service, Fort Collins, General Technical Report RM-GTR-277, 13–22
- Stoyan H, De-Polli H, Bohm S, Robertson GP, Paul EA (2000) Spatial heterogeneity of soil respiration and related properties at the plant scale. *Plant Soil* 222:203–214
- SURFER for Windows (1995) Release 6.01. Surface mapping system. Golden Software
- Wang G, Gertner G, Liu X, Anderson A (2001) Uncertainty assessment of soil erodibility factor for revised universal soil loss equation. *Catena* 46:1–14
- Wang G, Gertner G, Singh V, Shinkareva S, Parysow P, Anderson A (2002) Spatial and temporal prediction and uncertainty of soil loss using the revised universal soil loss equation: a case study of the rainfall-runoff erosivity R factor. *Ecol Model* 153:143–155
- Webster R (1985) Quantitative spatial analysis of soil in the field. In: Stewart BA (ed) Advances in soil science. Springer, New York
- Webster R, Oliver MA (1990) Statistical methods in soil and land resource survey. Oxford University Press, Oxford, p 316